Path-integral description of combined Hamiltonian and non-Hamiltonian dynamics in quantum dissipative systems

A. M. Barth,* A. Vagov, and V. M. Axt
Institut für Theoretische Physik III, Universität Bayreuth, 95440 Bayreuth, Germany
(Received 1 July 2016; revised manuscript received 5 September 2016; published 26 September 2016)

We present a numerical path-integral iteration scheme for the low-dimensional reduced density matrix of a time-dependent quantum dissipative system. Our approach simultaneously accounts for the combined action of a microscopically modeled pure-dephasing-type coupling to a continuum of harmonic oscillators representing, e.g., phonons, and further environmental interactions inducing non-Hamiltonian dynamics in the inner system represented, e.g., by Lindblad-type dissipation or relaxation. Our formulation of the path-integral method allows for a numerically exact treatment of the coupling to the oscillator modes and moreover is general enough to provide a natural way to include Markovian processes that are sufficiently described by rate equations. We apply this new formalism to a model of a single semiconductor quantum dot which includes the coupling to longitudinal acoustic phonons for two cases: (a) external laser excitation taking into account a phenomenological radiative decay of the excited dot state and (b) a coupling of the quantum dot to a single mode of an optical cavity taking into account cavity photon losses.

DOI: 10.1103/PhysRevB.94.125439

I. INTRODUCTION

Practically every quantum system experiences some kind of coupling to its environment and in many cases a realistic modeling requires the inclusion of quantum dissipative processes [1,2]. Such interactions with the environment typically lead to a decay of quantum mechanical coherence within the subsystem of interest that is known as decoherence or dephasing and often affects the dynamics in a non-negligible way. When the system-bath coupling becomes strong or when the environmental correlation decay becomes slow, it can be insufficient to treat the environment as a constant entity simply acting on the system but instead the reaction of the external degrees of freedom to the system dynamics also has to be considered. Accounting for these non-Markovian effects in a complete and correct way is not an easy task as besides the system dynamics also the finite bath-memory has to be incorporated in the equations of motion. A powerful and widely used method that allows such an exact treatment is provided by the path-integral approach [3–6], which exactly takes into account the environment excitations via the so-called influence functionals for the degrees of freedom of the quantum system [7]. This formalism has been applied in a variety of fields of both physics and chemistry such as energy transfer dynamics [8–16], Landau-Zener transitions [17,18], quantum mechanical Brownian motion [19], and semiconductor quantum dots with and without optical driving [20–25]. Moreover, it has been applied to systems with bosonic and fermionic baths [26,27], Ohmic and super-Ohmic [23] environments and can also be used to include multiple baths. However, in some cases the path-integral approach becomes impractical, because depending on the type of environmental interaction the influence functional cannot always be obtained easily. On the other hand, a completely microscopic description of the environment is not always necessary because many dissipative processes are well known to be correctly described in the Markov limit and a simplified or even parametric treatment of the environment is sufficient. In these cases a realistic modelling is usually achieved by simply adding phenomenological non-Hamiltonian contributions to the equations of motion of the reduced system as it is done, e.g., in the Lindblad formalism [2].

In this paper, we show that in a new generalized formulation the framework of the path-integral method allows to treat such non-Hamiltonian dynamics on equal footing with the Hamiltonian part of the equations of motion and can therefore also be used for models that describe some parts of the environment by phenomenological rates, while fully accounting for all non-Markovian effects induced by other couplings. This is not obvious, because the path-integral method usually relies on describing the dynamics in terms of the time-evolution operator, which yields purely Hamiltonian dynamics. More specifically here we present the path-integral formalism for a finite dimensional system that exhibits arbitrary non-Hamiltonian relaxation and a coupling to an arbitrary number of microscopic harmonic oscillator modes that is of the pure-dephasing type, i.e., the coupling does not induce transitions between the finite basis states. After defining the model and establishing our new formalism in Sec. II we apply it to a strongly confined semiconductor quantum dot coupled to a continuum of longitudinal acoustic phonons in Sec. III. The new method allows for an unbiased study of the interplay of the carrier-phonon coupling with the presence of radiative decay that is due to external field modes even in the regime of high temperatures and strong driving that is presented in Sec. III A. By exemplarily comparing the path-integral calculations with a Markovian master equation we also show that the new formalism can serve as an important benchmark tool. In Sec. III B, we then study the dynamics of a quantum dot coupled to a single photon mode inside a microcavity and compare the results with a previously developed hybrid approach. Finally, Sec. IV summarizes and concludes the paper.

*andreas.barth@uni-bayreuth.de

II. MODEL AND NUMERICAL METHOD

Our generic model consists of a few level system with a pure-dephasing type coupling to a continuum of harmonic oscillators. Further interactions between the few level system and the environment can be accounted for by additional non-Hamiltonian contributions to the equations of motion. The dynamics of the statistical operator for the total system consisting of the N states of the few level system belonging to the subspace $\mathcal{H}_N$ and the oscillatory modes belonging to the subspace $\mathcal{H}_{\rm osc}$ is given by the dynamical equation

$$\frac{d}{dt}\hat{\rho} = \frac{1}{i\hbar}\{\hat{H},\hat{\rho}\}_- + \mathcal{L}[\hat{\rho}], \tag{1}$$

where $\{.,.\}_-$ denotes the commutator. The Hamiltonian

$$\hat{H} = \hat{H}_N + \hat{H}_{\rm osc} \tag{2}$$

consists of an arbitrary N-dimensional time-dependent Hamiltonian $\hat{H}_N$ acting only on the N states $\{|\nu\rangle\} \in \mathcal{H}_N$ and

$$\hat{H}_{\rm osc} = \hbar\sum_j \omega_j \hat{b}_j^\dagger \hat{b}_j + \hbar\sum_{\nu j}\left(\gamma_j^\nu \hat{b}_j^\dagger + \gamma_j^{\nu *}\hat{b}_j\right)|\nu\rangle\langle\nu|, \tag{3}$$

which describes the interaction with the harmonic oscillators. Here, the symbol γ_j^ν denotes the coupling constant for the coupling between the state $|\nu\rangle$ and the bosonic mode j with energy $\hbar\omega_j$ that is created (destroyed) by $\hat{b}_j^\dagger$ ($\hat{b}_j$). Note that for simplicity, we treat the mode index j as being discrete even though the presented formalism can account for an arbitrary number of modes. The pure-dephasing type of the coupling often dominates for systems where the states of the few level system are energetically well separated such that inter-state transitions induced by the bosonic modes can be neglected.

While we denote Hilbert space operators with "hat" signs, the operator $\mathcal{L}[\hat{\rho}]$ appearing in Eq. (1) represents a Liouville space operator [28], i.e., a linear mapping between such operators, that allows the inclusion of non-Hamiltonian dynamics. In the following, we indicate such Liouville operators by putting the Hilbert space operator they act on into square brackets for clarity. Here, $\mathcal{L}[\hat{\rho}]$ is assumed to keep the parts of $\hat{\rho}$ belonging to the subspace $\mathcal{H}_{\rm osc}$ invariant and to only act on the few level system $\mathcal{H}_N$. We further assume that while $\mathcal{L}[\cdot]$ can be time-dependent, for simplicity it should be local in time. In principle, it would be possible to relax this assumption. However, depending on the memory depth of $\mathcal{L}[\cdot]$, this could increase the total memory time and thus the numerical cost of the path integral algorithm. Moreover, in many cases it is advisable to require certain conditions for the operator $\mathcal{L}[\cdot]$ such that important physical properties of the density matrix are preserved. All of these conditions mentioned above are enforced when $\mathcal{L}[\cdot]$ has the so called Lindblad form [2]

$$\mathcal{L}[\hat{\rho}] = \sum_i \gamma_i(t)\left(\hat{A}_i\hat{\rho}\hat{A}_i^\dagger - \frac{1}{2}\{\hat{\rho},\hat{A}_i^\dagger\hat{A}_i\}_+\right), \tag{4}$$

where the operators $\hat{A}_i$ represent operations within $\mathcal{H}_N$, the factors $\gamma_i(t)$ denote possibly time-dependent relaxation rates, and $\{.,.\}_+$ is the anticommutator. However, we would like to stress that the presented formalism does not depend on $\mathcal{L}[\cdot]$ to have this specific form.

Initially, the system is assumed to be in a product state of the states $\{|\nu\rangle\}$ and a thermal distribution of the oscillator modes $\hat{\rho}_{\rm th}$, i.e.,

$$\hat{\rho}(t=t_0) = \hat{\tilde{\rho}}(t=t_0)\otimes\hat{\rho}_{\rm th}. \tag{5}$$

The reduced density matrix of the N level subsystem

$$\hat{\tilde{\rho}}(t) = {\rm Tr}_{\rm osc}(\hat{\rho}(t)) \tag{6}$$

is obtained by tracing out all the degrees of freedom belonging to the subspace $\mathcal{H}_{\rm osc}$. In the following, we will derive a discretized representation of $\hat{\tilde{\rho}}(t)$ that is applicable for numerical calculation and does not require further approximations to the model given above.

A. Derivation of the path-integral solution

We start by separating the right-hand side of the master equation Eq. (1) into two Liouville operators $\mathcal{L}_N[\cdot]$ and $\mathcal{L}_{\rm osc}[\cdot]$ that are given by

$$\mathcal{L}_N[\hat{\rho}] = \frac{1}{i\hbar}\{\hat{H}_N,\hat{\rho}\}_- + \mathcal{L}[\hat{\rho}], \tag{7}$$

$$\mathcal{L}_{\rm osc}[\hat{\rho}] = \frac{1}{i\hbar}\{\hat{H}_{\rm osc},\hat{\rho}\}_-, \tag{8}$$

and write the master equation as

$$\frac{d}{dt}\hat{\rho} = \mathcal{L}_N[\hat{\rho}] + \mathcal{L}_{\rm osc}[\hat{\rho}]. \tag{9}$$

Keeping the accuracy linear in a small time step Δt the propagation of the statistical operator to a time $t+\Delta t$ can be performed by applying $\mathcal{L}_N[\cdot]$ and $\mathcal{L}_{\rm osc}[\cdot]$ subsequently and we can write

$$\hat{\rho}(t+\Delta t) = \hat{U}\mathcal{M}_t[\hat{\rho}(t)]\hat{U}^\dagger + \mathcal{O}(\Delta t^2). \tag{10}$$

Here, we have used the fact that the dynamics described by $\mathcal{L}_{\rm osc}[\cdot]$ is purely Hamiltonian and therefore can be expressed in terms of the time evolution operator

$$\hat{U} = \exp\left(-\frac{i}{\hbar}\hat{H}_{\rm osc}\Delta t\right). \tag{11}$$

Further, we have introduced the time-ordered operator

$$\mathcal{M}_t[\cdot] = \mathcal{T}\exp\left(\int_t^{t+\Delta t}\mathcal{L}_N dt'\right)[\cdot], \tag{12}$$

which acts as a generalized time evolution operator that describes the evolution of the few level system including the non-Hamiltonian part of the dynamics in the absence of the oscillator coupling from time t to $t+\Delta t$. Importantly, the representation of these operators in terms of the matrix exponentials fulfills the necessary conservation requirements at each time step, such as a unitary evolution for the Hamiltonian dynamics.

We can now use the relation Eq. (10) recursively to find an expression for the statistical operator at time t starting from the initial time t_0. By inserting several identity operators $\sum_\nu |\nu\rangle\langle\nu|$ acting on $\mathcal{H}_N$ at different time steps $t_l = t_0 + l\Delta t$, where the summation $\sum_\nu$ runs over all states of the few level system, we

arrive at a discretized representation

$$\hat{\rho}_{\nu_n\mu_n} = \sum_{\substack{\nu_0\ldots\nu_{n-1}\\ \mu_0\ldots\mu_{n-1}}} \hat{U}_{\nu_n}\ldots\hat{U}_{\nu_1}\hat{\rho}_{\nu_0\mu_0}\hat{U}^{\dagger}_{\mu_1}\ldots\hat{U}^{\dagger}_{\mu_n} \prod_{l=1}^{n}\mathcal{M}^{\nu_{l-1}\mu_{l-1}}_{\nu_l\mu_l} \tag{13}$$

for the matrix elements of the statistical operator, which we denote by

$$\hat{\rho}_{\nu_l\mu_l} = \langle\nu_l|\hat{\rho}(t_l)|\mu_l\rangle. \tag{14}$$

We have written

$$\hat{U}_{\nu} = \langle\nu|\hat{U}|\nu\rangle \tag{15}$$

for the diagonal elements of the time-evolution operator $\hat{U}$ that are operators acting on the subspace $\mathcal{H}_{\rm osc}$ and also introduced the symbol

$$\mathcal{M}^{\nu_{l-1}\mu_{l-1}}_{\nu_l\mu_l} = \langle\nu_l|\mathcal{M}_t[|\nu_{l-1}\rangle\langle\mu_{l-1}|]|\mu_l\rangle, \tag{16}$$

which represents the matrix elements of the operator that results when $\mathcal{M}_t$ is applied to the canonical basis operator $|\nu_{l-1}\rangle\langle\mu_{l-1}|$.

We can now use the results of previous work [23] where using a path-integral method and a representation of the oscillatory modes in terms of coherent states the trace over the oscillators for an operator of the same form as the one in Eq. (13) has been performed. Tracing out in this way the oscillator degrees of freedom we finally obtain the elements of the reduced density matrix $\hat{\bar{\rho}}$ at the nth time step

$$\bar{\rho}_{\nu_n\mu_n} = \mathrm{Tr}_{\rm osc}\left(\hat{\rho}_{\nu_n\mu_n}\right) = \sum_{\substack{\nu_0\ldots\nu_{n-1}\\ \mu_0\ldots\mu_{n-1}}} \bar{\rho}_{\nu_0\mu_0}\exp\left(S^{\mu_n\ldots\mu_1}_{\nu_n\ldots\nu_1}\right)\prod_{l=1}^{n}\mathcal{M}^{\nu_{l-1}\mu_{l-1}}_{\nu_l\mu_l}, \tag{17}$$

where all summations run over the N states of $\mathcal{H}_{\mathcal{N}}$ and the influence functional $S^{\mu_n\ldots\mu_1}_{\nu_n\ldots\nu_1}$ incorporates the memory of the oscillator modes in the dynamics of the few-level system. For simplicity, here, we only give the expression for the influence functional for the special case where the coupling constants γ^{ν}_j are all either purely real or purely imaginary. A more general representation for the influence functional that does not make use of this assumption can be found in Ref. [23]. The functional reads

$$S^{\mu_n\ldots\mu_1}_{\nu_n\ldots\nu_1} = \sum_{l=1}^{n}\sum_{l'=1}^{l} S_{\nu_l\nu_{l'}\mu_l\mu_{l'}} \tag{18}$$

with

$$S_{\nu_l\nu_{l'}\mu_l\mu_{l'}} = -K_{\nu_{l'}\nu_l}(t_l - t_{l'}) - K^{*}_{\mu_l\mu_{l'}}(t_l - t_{l'}) + K^{*}_{\nu_l\mu_{l'}}(t_l - t_{l'}) + K_{\nu_{l'}\mu_l}(t_l - t_{l'}) \tag{19}$$

and the memory kernels

$$K_{\nu_l\mu_{l'}}(\tau) = 2\int_0^{\infty} d\omega\frac{J_{\nu_l\mu_{l'}}(\omega)}{\omega^2}(1-\cos(\omega\Delta t)) \times\left[\coth\left(\frac{\hbar\omega}{2k_BT}\right)(\cos(\omega\tau)) - i\sin(\omega\tau)\right] \tag{20}$$

and

$$K_{\nu_l\mu_l}(0) = \int_0^{\infty} d\omega\frac{J_{\nu_l\mu_l}(\omega)}{\omega^2}\times\left[\coth\left(\frac{\hbar\omega}{2k_BT}\right) \times(1-\cos(\omega\Delta t)) + i\sin(\omega\Delta t) - i\omega\Delta t\right] \tag{21}$$

where we have introduced the spectral density

$$J_{\nu\mu}(\omega) = \sum_j \gamma^{\nu}_j\gamma^{\mu *}_j\delta(\omega-\omega_j). \tag{22}$$

It should be noted that the last term in Eq. (21) induces a polaronic shift of the energy levels of the few-level system.

B. Evaluation of the path-integral expression

Obtaining the reduced density matrix at the nth time step from Eq. (17) requires the summation over N^{2n} single contributions, which quickly becomes unfeasible even for very small N. Each of the single summands represents a possible *path*, i.e., a trajectory through the subspace $\mathcal{H}_N\otimes\mathcal{H}_N$ given by the configurations at each time-step $(\nu_n,\mu_n)\ldots(\nu_1,\mu_1)$, which is the reason that the summation scheme is called a numerical path-integration method. To efficiently use this expression also for the iteration over many time-steps it is necessary to exploit the finite memory time of the system of oscillator modes that is reflected by a finite decay time of the memory kernels [Eqs. (20) and (21)]. This allows a truncation of the influence functional $S^{\mu_n\ldots\mu_1}_{\nu_n\ldots\nu_1}$, efficiently making it only depend on the states of the n_c most recent time-steps $(\nu_n,\mu_n)\ldots(\nu_{n-n_c+1},\mu_{n-n_c+1})$. Such a truncation can be exploited by combining the path-integral method with the augmented density matrix approach [4,5], which applies also in the present case when including non-Hamiltonian dynamics. The augmented density matrix can be thought of as a $2n_c$ dimensional tensor of weights for the different possible configurations of the most recent n_c time steps and can be calculated iteratively in each time step following the relation

$$\rho^{\mu_n\ldots\mu_{n-n_c+1}}_{\nu_n\ldots\nu_{n-n_c+1}} = \mathcal{M}^{\nu_{n-1}\mu_{n-1}}_{\nu_n\mu_n} \times\sum_{\substack{\nu_{n-n_c}\\ \mu_{n-n_c}}}\exp\left(S^{\mu_n\ldots\mu_{n-n_c}}_{\nu_n\ldots\nu_{n-n_c}}\right)\rho^{\mu_{n-1}\ldots\mu_{n-n_c}}_{\nu_{n-1}\ldots\nu_{n-n_c}}. \tag{23}$$

This explicit iteration yields a numerical effort that is linear in the total number of time steps and requires the calculation and storage of only N^{2n_c} (compared to N^{2n}) weights and thus removes the restriction to a limited number of iteration steps in Eq. (17) that we mentioned above.

The decay time of the memory kernels is determined by the spectral density of the harmonic oscillator coupling $J(\omega)$, which can be classified by its low-frequency behavior into sub-Ohmic coupling where $J(\omega)\sim\omega^a$ with $a<1$ as $\omega\to 0$, Ohmic coupling where $a=1$ and super-Ohmic coupling where $a>1$. The Ohmic case marks the borderline between a sub-Ohmic environment inducing exponential relaxations and the super-Ohmic case which is characterized by non-exponential typically only partial relaxations that entail a variety of non-Markovian dynamical effects [3]. The presented formalism can also deal with the latter super-Ohmic case [23] that is realized in the examples in this article for the coupling of acoustic phonons in a crystal solid where $a=3$.

Finally, we would like to note that the inclusion of non-Hamiltonian dynamics in Eq. (1) does not increase the required memory depth n_c compared to the case of purely Hamiltonian dynamics as long as the former part of the dynamics does not involve a memory time that is longer than the one induced by the harmonic oscillator coupling. Here, this is obviously fulfilled as the operator $\mathcal{L}[\cdot]$ in Eq. (1) is assumed to be local in time. Notably, this also means that the numerical cost is practically not increased by adding non-Hamiltonian contributions.

III. APPLICATION: DYNAMICS OF A SEMICONDUCTOR QUANTUM DOT

In this section, we utilize the extended path-integral formalism to calculate the dynamics of an optically coupled strongly confined semiconductor quantum dot (QD) and also compare the results with those of some established methods. For circularly polarized light with a central frequency close to the excitonic resonance, a QD can be described for many purposes in good approximation as a two-level system consisting of the crystal ground-state $|0\rangle$ and an exciton state $|X\rangle$ with energy $\hbar\omega_X$ given by the Hamiltonian

$$\hat{H}_{\mathrm{QD}} = \hbar\omega_X |X\rangle\langle X|. \tag{24}$$

Apart from the optically induced coherent dynamics which we will describe specifically in the corresponding two subsections also the coupling to the lattice vibrations of the surrounding solid state material needs to be taken into account. For the strongly confined GaAs-based QD considered here the deformation potential coupling to longitudinal acoustic (LA) phonons represents the predominant impact of the phonon environment [29] and has the same form as Eq. (3) where the index j refers to the wave vector $\mathbf{q}$ of the LA phonon modes. The coupling constants $\gamma_{\mathbf{q}}^{\nu}$ are given by $\gamma_{\mathbf{q}}^{0} = 0$ for the ground state and $\gamma_{\mathbf{q}}^{1} = \gamma_{\mathbf{q}}^{e} - \gamma_{\mathbf{q}}^{h}$ for the exciton state with

$$\gamma_{\mathbf{q}}^{e(h)} = \Psi^{e(h)}(\mathbf{q}) \frac{|\mathbf{q}| D_{e(h)}}{\sqrt{2V\rho\hbar\omega_{\mathbf{q}}}} \tag{25}$$

being the coupling constants for the electron (e) and hole (h) coupling to the $\mathbf{q}$ phonon mode. Here, the form factors $\Psi^{e(h)}$ are assumed to be spherically symmetric and Gaussian as applies for a parabolic confinement potential and the deformation potential constants $D_e = 7.0$ eV and $D_h = -3.5$ eV, the mass density $\rho = 5370$ kg/m^3 as well as the sound velocity $c_s = 5110$ m/s for GaAs are taken from the literature [30]. The mode volume V simply represents a normalization constant for the summation over the phonon modes in Eq. (3). The spectral density of the phonon coupling given in Eq. (22) is only nonvanishing for $\nu = \mu = 1$ and in this case reads

$$J_{11}(\omega) = \frac{\omega^3}{4\pi^2\rho\hbar c_s^5}\left(D_e e^{-\omega^2 a_e^2/(4c_s^2)} - D_h e^{-\omega^2 a_h^2/(4c_s^2)} 77\right)^2, \tag{26}$$

where the sound velocity enters via the linear phonon dispersion relation $\omega_{\mathbf{q}} = c_s|\mathbf{q}|$ and $a_{e(h)}$ denote the root mean square of the Gaussian wave function extensions of the electron and hole, respectively. Here we set $a_e = 4.0$ nm, which can be interpreted as the QD radius and set a_e/a_h to 1.15.

We would like to point out that there have been many suggestions to simulate the QD dynamics under the influence of the carrier-phonon interaction outlined above including correlation expansions [31,32], analytical solutions for delta excitation [33], an exact diagonalization approach [34], quantum jump approaches [35] and various forms of master equations [36–42] some of which account for contributions of arbitrarily high order in the dot-phonon coupling with the help of the polaron transformation [22,43–46]. This variety of methods is also a result of the many different optical excitation scenarios that are discussed for QDs which can range from weak cavity couplings to strong pulsed laser excitation. The path integral approach presented here provides a numerical scheme that allows to deal with all of these situations without introducing further approximations to the model formulated above.

A. Laser-driven quantum dot with radiative decay

As a first example for an application of our new method we consider the QD dynamics that is driven by an external laser field and affected by both the phonon-induced relaxation and the radiative decay of the exciton state that reduces the exciton lifetime. As the radiative decay is known to be reasonably described as a Markov process in a good approximation it can be included by a Lindblad contribution to the master equation. In the rotating frame, the contribution to the Hamiltonian for the laser driven QD reads after applying the common dipole and rotating wave approximations

$$\hat{H}_{\text{dot-light}} = \tfrac{1}{2}\hbar f(t)\big(|0\rangle\langle X| + |X\rangle\langle 0|\big) - \Delta|X\rangle\langle X|, \tag{27}$$

where $f(t)$ is the envelope function of the laser field referred to as field strength and Δ is the detuning of the laser from the polaron-shifted exciton resonance. The radiative decay of the exciton state is treated as a phenomenologically damping rate accounted for by a Lindblad type operator in the form of Eq. (4) with a single transition $\hat{A}_1 = |0\rangle\langle X|$ and a corresponding damping rate γ (cf. Ref. [45]).

Figure 1 shows the time-dependent exciton occupation of the QD under resonant and off-resonant cw excitation as indicated. In the absence of the phonon interaction (left column) our computational scheme exactly reproduces known analytical results exhibiting damped Rabi oscillations. For off-resonant excitation [cf. panel (c)], of course, the amplitude of the oscillations is reduced and the Rabi frequency is increased as can be seen in Fig. 1(c). The radiative decay also influences the stationary exciton occupation for $\gamma > 0$, which is given by [47]

$$C^{\infty}_{X,\text{noph.}} = \frac{f^2}{2f^2 + \gamma^2 + (2\Delta/\hbar)^2} \tag{28}$$

and decreases from its maximum value of 0.5 with an increasing damping rate and an increasing detuning. This simple application without the phonon interaction serves as a proof of principle that the formalism presented here correctly incorporates non-Hamiltonian dynamics of Lindblad-type within the framework of the path-integral method.

In the other limiting case where $\gamma = 0$, but the phonon coupling is included the results obtained from the presented formalism coincide with previous path-integral calculations [23]

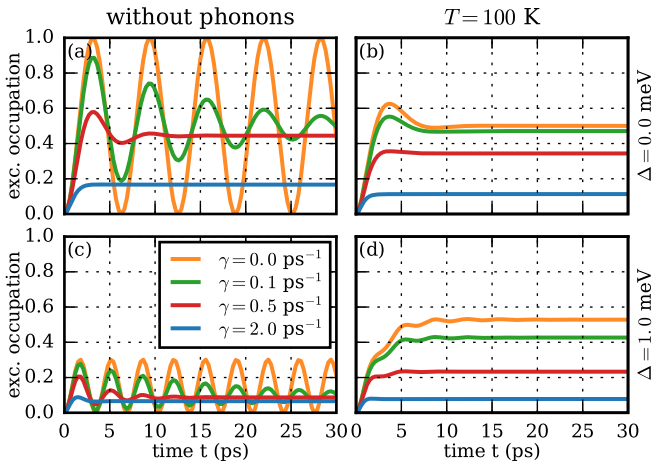

FIG. 1. Time-dependent exciton occupation C_X of a QD calculated by the path-integral formalism for constant driving with field strength $f = 1.0\ \mathrm{ps}^{-1}$ for resonant [(a) and (b)] and detuned [(c) and (d)] excitation ($\Delta = 1.0$ meV) for different values of the radiative decay rate (see legend). Left column: without phonon interaction, right column: including phonon interaction at temperature $T = 100$ K in addition to the radiative decay.

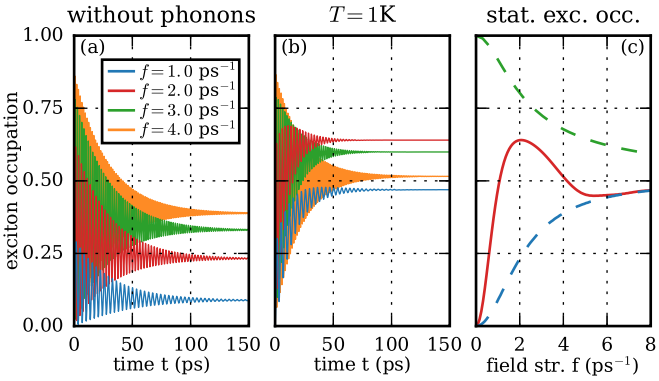

FIG. 2. Time-dependent exciton occupation C_X of a QD for off-resonant ($\Delta = 1.0$ meV) cw excitation for different field strengths (see legend) including radiative decay ($\gamma = 0.05\ \mathrm{ps}^{-1}$) without the phonon-interaction (a) and including phonons at temperature $T = 1$ K (b). (c) Stationary exciton occupation reached at long times when only the phonon interaction is present (green, dashed), when only the radiative decay is present (blue, dashed) and when both relaxation mechanisms are present (red, solid).

that did not yet allow to account for any non-Hamiltonian dynamics. This can be seen explicitly from the orange curve for $\gamma = 0$ in the right column of Fig. 1 where calculations that include the phonon coupling for a temperature of $T = 100$ K are shown. As known from previous simulations at such high temperatures the Rabi oscillations are almost completely damped by the phonon scattering.

As for the radiative damping also the phonon coupling strongly affects the stationary value of the exciton occupation that is reached at long times. It can be seen that for fixed γ the stationary value C_X^∞ is slightly decreased by the phonon coupling for resonant excitation while it is increased for off-resonant excitation. The reason for this is that while the radiative decay always drives the QD towards the ground state and thus away from the exciton, off-resonant excitation with positive detuning enables phonon-assisted transitions between the laser dressed states that yield a higher exciton occupation [41,46,48–53]. As it can be seen in Fig. 1, this feature prevails when the phonon induced relaxation between photon dressed states is combined with the radiative decay of the exciton state discussed here.

Figure 2 shows the combined influence of the radiative decay and the phonon-interaction by plotting the time-dependent exciton occupation under positively detuned cw excitation for different field strengths as indicated. Without the phonon interaction [panel (a)] the stationary exciton occupation that is reached at long times C_X^∞ always stays below 0.5 and rises with increasing field strength as it was expected from Eq. (28). Interestingly, when including the phonon scattering [panel (b)] the stationary exciton occupation no longer depends on the field strength in a monotonic way. To analyze this in more detail, we have plotted C_X^∞ as a function of the field strength in Fig. 2(c) (red, solid) together with corresponding results for the two limiting cases where only the phonon scattering (dashed, green) or only the radiative decay (dashed, blue) has been accounted for. In case of the complete dynamic, there is a clear maximum around $f = 2.0\ \mathrm{ps}^{-1}$ and a local minimum around $f = 5.0\ \mathrm{ps}^{-1}$ and overall the full model predicts very different features compared to the two limiting cases. This behavior originates from the combination effects between the radiative decay and the phonon-induced relaxation as will be explained in the following. For very small field strengths, e.g., below $f = 0.5\ \mathrm{ps}^{-1}$, the timescale of the phonon-induced relaxation [54] is long compared to the radiative decay rate and therefore one might expect the phonon coupling to play a subordinate role. However, in this regime, the QD state targeted by the phonon-induced relaxation has an especially strong excitonic character [24], which without radiative decay would result in an exciton occupation near one towards very long times [54]. This can be seen by the dashed green line where the exciton occupation approaches one in the limit $f \to 0^+$, but of course, in the absence of any optical coupling, i.e., at exactly $f = 0$, the system remains in its ground state. When the radiative decay is included a remainder of this strong effect is still visible and thus leads to a clear difference between the results with (red, solid) and without phonons (blue, dashed) even for low field strengths. For larger values of f the phonon-induced relaxation becomes more effective yielding a steep increase of C_X^∞ and values well above 0.5 that would not be expected from the radiative decay alone. Beyond the maximum at $f = 2.0\ \mathrm{ps}^{-1}$, C_X^∞ decreases again as the QD state targeted by the phonon relaxation becomes less excitonic in character and even more importantly the phonon-coupling becomes less efficient again because the phonon environment is too sluggish to follow the rapid dynamics of the QD [21,55]. At very large $f > 5.0\,\mathrm{ps}^{-1}$ the phonon coupling no longer has a significant impact on C_X^∞ and the stationary exciton occupation is almost entirely dominated by the radiative decay resulting in a local minimum and a subsequent slow increase towards 0.5. It is worth noting that the nonmonotonic dependence of the damping of the Rabi oscillations that is due to the phonon

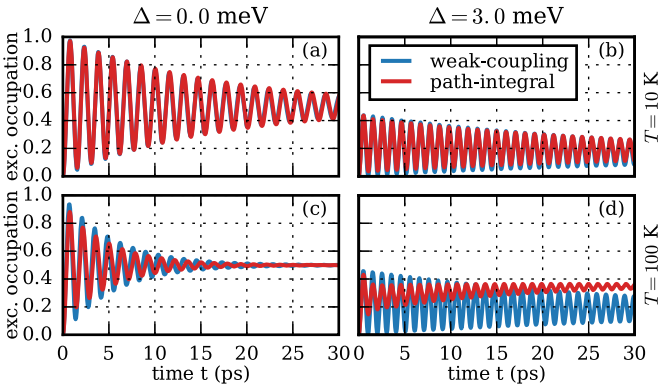

FIG. 3. Comparison of the time-dependent exciton occupation of a QD for resonant (left) and detuned (right) cw excitation calculated by the path-integral method (red) and the weak coupling theory (blue). The radiative decay rate has been set to $\gamma = 0.05\ \mathrm{ps}^{-1}$ and a relatively high field strength of $f = 4.0\ \mathrm{ps}^{-1}$ was chosen.

coupling persists under the influence of the radiative decay as it can be seen from Fig. 2(b).

A strong advantage of the numerical path-integral method is that because of the exact treatment of the model discussed here it can be used to benchmark perturbative approaches and explore their range of validity. To this end, we have compared our results with those of a Markovian master equation that treats the phonon coupling up to second order which we took from the literature [42] and that also allows an inclusion of the radiative exciton decay considered here. Figure 3(a) shows the damped Rabi oscillations of the exciton occupation under constant resonant excitation by a strong electric field ($f = 4.0\ \mathrm{ps}^{-1}$) under the influence of the phonon coupling ($T = 10$ K) and the radiative decay ($\gamma = 0.05\ \mathrm{ps}^{-1}$). As it can be expected at such low temperatures the weak-coupling theory (blue) works very well and the predicted dynamics of the exciton occupation is practically identical with those of the path-integral method (red), which indicates that in this parameter range non-Markovian effects and multiphonon processes that the weak-coupling theory cannot capture are of minor importance. Notably, the close match between the two methods is an important further verification of the correctness of the presented path-integral algorithm with Lindblad-type relaxation. When raising the temperature to $T = 100$ K, cf. Fig. 3(c), some differences between the results of the path-integral calculations and the weak-coupling theory become visible. The phonon-induced damping is slightly underestimated by the weak-coupling theory and also there is a slight discrepancy of the predicted Rabi frequency renormalization between the two methods. However, considering the very high temperature, the Master equation still yields reasonable results. This is due to the strong driving chosen here while for slower driving it is well known that the weak coupling theory can not account for the strong Rabi frequency renormalization [22] and even can yield unphysical results at very high temperatures [42]. For off-resonant excitation, the path-integral calculations again practically coincide with those obtained from the Master equation approach at $T = 10$ K [panel (b)]. However, at higher temperatures, cf. Fig. 3(d), strong differences between the two approaches become visible. The phonon-induced damping is clearly underestimated by the weak-coupling theory and even more important the stationary exciton occupation at long times predicted by the weak-coupling theory is considerably lower than the value predicted by the path-integral calculations. The regime of strong driving at elevated temperatures is especially difficult to deal with in the Master equation approach. Because the path-integral method does not rely on any approximations regarding the order of the phonon coupling or the optical driving that it accounts for and is only limited by the errors introduced by the discretization of the time axis, it provides an important benchmark. Most importantly, the regime of strong driving must be considered when simulating pulsed excitation scenarios in which high field strengths can be reached and that are often required to reproduce experimental results.

B. QD coupled to a single cavity mode

Another system that can be described within the combined Lindblad and path-integral method is a QD inside an optical cavity. Here, we assume that the quantized cavity photon modes are sufficiently separated in frequency such that only a single mode effectively couples to the QD. Further, we assume that the system can be described in the single-photon limit where only states with zero or one cavity photon have to be considered. Besides the coupling to LA phonons that is independent of the cavity coupling also photon losses that are due to imperfections of the cavity mirrors are highly relevant for the system dynamics. Similar to the previous examples we model the dynamics of the QD consisting of two electronic levels coupled to the cavity mode and the phonon subsystem in an exact Hamiltonian way while we attribute the cavity losses to the part of the environment that is described by rate equations. In the rotating frame the Hamiltonian for the QD coupled to the cavity mode is described via the Jaynes-Cummings model and reads after applying the common dipole and rotating wave approximations

$$\hat{H}_{\text{dot-cav}} = \hbar g(|P\rangle\langle X| + |X\rangle\langle P|) - \Delta|X\rangle\langle X|, \qquad (29)$$

where g is the light-matter coupling strength, Δ is the detuning of the cavity-mode from the polaron-shifted exciton resonance, and the two-level electronic basis of the QD-cavity system consists of the state $|P\rangle$ with the QD in the ground-state and one cavity photon and the exciton state $|X\rangle$ without a cavity photon. Only $|X\rangle$ couples to the phonon enivironment and the coupling is the same as in the previous examples. The photon losses of the cavity are modelled by a relaxation with rate κ from $|P\rangle$ to the state where the QD is in its ground-state and no photon is present $|G\rangle$ which is accounted for by a Lindblad contribution to the equation of motion for the reduced density matrix [45] by setting $\hat{A}_1 = |G\rangle\langle P|$ in Eq. (4).

Figure 4 shows the occupation of the excited state $|X\rangle$ as a function of time for a system initially prepared in the excited state for a cavity-loss rate $\kappa = 0.1\ \mathrm{ps}^{-1}$ at two different temperatures for resonant and off-resonant coupling (see caption). For resonant coupling we can see Rabi oscillations with a decreasing amplitude, which can be attributed to the cavity losses. Similar oscillations can also be seen for off-resonant coupling, but in this case a positive detuning (red) leads to a strongly increased exciton decay time compared

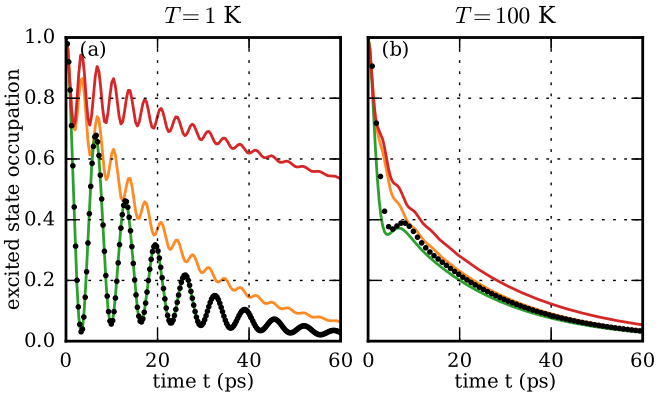

FIG. 4. Time-dependent occupation of the excited state C_X of a QD inside a cavity for resonant (green) and off-resonant (red: $\Delta = 1.0$ meV, orange: $\Delta = -1.0$ meV) coupling. The black dots show the results of a hybrid approach that is only applicable in the resonant case (see text). (Left) $T = 1$ K. (Right) $T = 100$ K. $\kappa = 0.1$ ps^{-1}.

to a negative detuning (orange). This asymmetry has already been discussed in Ref. [45] and is due to the fact that at low temperatures phonon emission process dominate absorption processes, and in fact at a higher temperature (right panel), this asymmetry disappears. Here we have chosen to repeat these kind of calculations to show that temperatures as high as $T = 100$ K can easily be accessed using the path-integral approach, which is hard to reach with other methods. Previously, the present model of a QD-cavity system has also been treated by a hybrid approach [56], which requires the knowledge of the phonon-induced Rabi-frequency renormalization and the strength of the phonon-induced damping in the absence of cavity losses. These input parameters can be gained by analyzing the damped oscillations of the excited state occupation in a lossless cavity occurring for constant resonant coupling as it can be calculated using the path-integral formalism in its previous formulation [23,57]. In the hybrid approach this input is then combined with an *a posteriori* phenomenological treatment of the cavity losses. Thus, even though this way the damping and the frequency renormalization are calculated in a nonperturbative way, the hybrid approach does not yet treat the cavity losses and the phonon coupling on equal footing as the combined Lindblad and path-integral approach does. Moreover, the derivation of the hybrid approach in Ref. [56] made explicit use of special properties that are only fulfilled for constant resonant excitation. Therefore the present work also drastically extends the parameter range accessible with the path-integral approach if one needs to include the effects of cavity losses, which in many cases play a crucial role for the system dynamics. Here, we have compared the results obtained from the hybrid approach for resonant excitation, shown as black dots in Fig. 4, with the path-integral method for both temperatures. For low temperatures the results are identical, while at higher temperature small deviations become visible. Similar to our previous comparison with the weak-coupling theory also here the path-integral method serves as an excellent benchmark to explore the limits of the applicability of less rigorous methods.

IV. CONCLUSIONS

We have presented an extension to the numerical path-integral formalism previously used to calculate the reduced density matrix of a time-dependent few level system coupled to a set of harmonic oscillator modes that allows a natural and systematic inclusion of non-Hamiltonian dynamics within the path integral framework. Our combined method shows a way how to go beyond the representation of the path-integral formalism that relies on using the time-evolution operator and thus can be used to add arbitrary linear operations acting on the reduced density matrix to the equations of motion. We applied this new method to an optically coupled semiconductor quantum dot (QD) where the coupling to longitudinal acoustic phonons is treated nonperturbatively for different optical excitation conditions and different environmental effects that are described in the Markov limit by corresponding phenomenological rates. The combined Lindblad and path-integral method turns out to be a highly valuable tool for the treatment of optically coupled QDs with strong phonon interaction and similar quantum dissipative systems for a number of reasons. First of all, it allows to treat the deformation potential coupling to longitudinal acoustic phonons, which has been identified as the major decoherence mechanism in strongly confined QDs, in a numerically exact way that includes multiphonon processes and all non-Markovian effects. This makes it possible to explore the regimes of arbitrarily strong QD-phonon coupling and both low and high temperatures in a nonperturbative way. Here, it is worth noting that within the path integral approach higher temperatures are actually easier to deal with as the memory time becomes shorter and thus less memory steps are needed while the scope of some approximate methods that explicitly truncate the phonon subspace is restricted to lower temperatures. Besides the phonon coupling also the optical excitation can be chosen arbitrarily as the formalism is able to deal with both weak and strong driving, constant and pulsed excitation and also rapid changes of the excitation parameters that can prevent an adiabatic evolution of the coupled light-matter system. This also includes situations with chirped excitation or with multiple overlapping pulses of different frequency where the introduction of a suitable basis of photon-dressed states as needed by some schemes becomes nonobvious as the rotating frames naturally associated with each pulse differ. Moreover, the method can be used to calculate all elements of the reduced density matrix in the original frame of reference which not only gives access to the QD occupations, but also to the coherences of the reduced system. The inclusion of processes described by rate equations within the path-integral formalism that is made possible by the present work allows taking into account other loss channels that are relevant in typical experimental situations involving QDs. For example, the presented method has already been successfully used to include electron tunneling effects in photocurrent measurements using off-resonant two-pulse and two-color excitation [58,59].

In our first application, we discussed the combined effects of the radiative decay and the phonon scattering on the driven stationary nonequilibrium state of a two-level QD for both resonant and off-resonant excitation showing that there is a nonmonotonic dependence of the stationary exciton

occupation on the driving strength. This is not expected in both limiting cases where either the dot phonon interaction or the radiative decay provide the only environment coupling. So far no unbiased approach was formulated for studying such combination effects. We then used the path-integral results to explore the range of validity of a weak-coupling method that treats the phonon coupling perturbatively and found for strong driving in the regime of detuned excitation at high temperatures significant deviations between the two methods while otherwise the weak-coupling theory works well over wide parameter ranges. Finally, we applied our new formalism to the case of a QD coupled to a single cavity mode and analyzed the exciton lifetime that is limited due to photon losses of the cavity for different detunings of the optical mode from the QD resonance at low and very high temperatures. The combined Lindblad and path-integral method has also been used as a benchmark to test a previously developed hybrid approach that was limited to resonant excitation.

ACKNOWLEDGMENTS

A.M.B. and V.M.A. gratefully acknowledge the financial support from Deutsche Forschungsgemeinschaft via the Project No. AX 17/7-1.

[1] U. Weiss, *Quantum Dissipative Systems*, 2nd ed. (World Scientific, Singapore, 1999).
[2] H. P. Breuer and F. Petruccione, *The Theory of Open Quantum Systems*, 1st ed. (Oxford University Press, Oxford, 2002).
[3] A. J. Leggett, S. Chakravarty, A. T. Dorsey, M. P. A. Fisher, A. Garg, and W. Zwerger, Rev. Mod. Phys. **59**, 1 (1987).
[4] N. Makri and D. Makarov, J. Chem. Phys. **102**, 4600 (1995).
[5] N. Makri and D. Makarov, J. Chem. Phys. **102**, 4611 (1995).
[6] N. Makri, J. Chem. Phys. **141**, 134117 (2014).
[7] R. P. Feynman and F. Vernon, Ann. Phys. (NY) **24**, 118 (1963).
[8] P. Nalbach, A. Ishizaki, G. R. Fleming, and M. Thorwart, New J. Phys. **13**, 063040 (2011).
[9] P. Nalbach and M. Thorwart, J. Chem. Phys. **132**, 194111 (2010).
[10] P. Nalbach, J. Eckel, and M. Thorwart, New J. Phys. **12**, 065043 (2010).
[11] J. Eckel, J. H. Reina, and M. Thorwart, New J. Phys. **11**, 085001 (2009).
[12] M. Thorwart, J. Eckel, J. H. Reina, P. Nalbach, and S. Weiss, Chem. Phys. Lett. **478**, 234 (2009).
[13] P. Nalbach, A. J. A. Achner, M. Frey, M. Grosser, C. Bressler, and M. Thorwart, J. Chem. Phys. **141**, 044304 (2014).
[14] H. Kim, O. Choi, and E. Sim, J. Phys. Chem. C **114**, 20394 (2010).
[15] J. Lee, O. Choi, and E. Sim, J. Phys. Chem. Lett. **3**, 714 (2012).
[16] X.-T. Liang, W.-M. Zhang, and Y.-Z. Zhuo, Phys. Rev. E **81**, 011906 (2010).
[17] P. Nalbach and M. Thorwart, Phys. Rev. Lett. **103**, 220401 (2009).
[18] S. Javanbakht, P. Nalbach, and M. Thorwart, Phys. Rev. A **91**, 052103 (2015).
[19] M. Thorwart, P. Reimann, and P. Hänggi, Phys. Rev. E **62**, 5808 (2000).
[20] M. Thorwart, J. Eckel, and E. R. Mucciolo, Phys. Rev. B **72**, 235320 (2005).
[21] A. Vagov, M. D. Croitoru, V. M. Axt, T. Kuhn, and F. M. Peeters, Phys. Rev. Lett. **98**, 227403 (2007).
[22] D. P. S. McCutcheon, N. S. Dattani, E. M. Gauger, B. W. Lovett, and A. Nazir, Phys. Rev. B **84**, 081305(R) (2011).
[23] A. Vagov, M. D. Croitoru, M. Glässl, V. M. Axt, and T. Kuhn, Phys. Rev. B **83**, 094303 (2011).
[24] M. Glässl, A. Vagov, S. Lüker, D. E. Reiter, M. D. Croitoru, P. Machnikowski, V. M. Axt, and T. Kuhn, Phys. Rev. B **84**, 195311 (2011).
[25] M. Glässl, A. M. Barth, and V. M. Axt, Phys. Rev. Lett. **110**, 147401 (2013).
[26] D. Segal, A. J. Millis, and D. R. Reichman, Phys. Rev. B **82**, 205323 (2010).
[27] L. Simine and D. Segal, J. Chem. Phys. **138**, 214111 (2013).
[28] S. Mukamel, *Principles of Nonlinear Optical Spectroscopy*, 1st ed. (Oxford University Press, New York, 1995).
[29] B. Krummheuer, V. M. Axt, and T. Kuhn, Phys. Rev. B **65**, 195313 (2002).
[30] B. Krummheuer, V. M. Axt, T. Kuhn, I. D'Amico, and F. Rossi, Phys. Rev. B **71**, 235329 (2005).
[31] J. Förstner, C. Weber, J. Danckwerts, and A. Knorr, Phys. Rev. Lett. **91**, 127401 (2003).
[32] A. Krügel, V. M. Axt, and T. Kuhn, Phys. Rev. B **73**, 035302 (2006).
[33] A. Vagov, V. M. Axt, and T. Kuhn, Phys. Rev. B **66**, 165312 (2002).
[34] P. Kaer, P. Lodahl, A.-P. Jauho, and J. Mork, Phys. Rev. B **87**, 081308 (2013).
[35] N. Renaud and F. C. Grozema, Phys. Rev. B **90**, 165307 (2014).
[36] A. Nazir, Phys. Rev. B **78**, 153309 (2008).
[37] A. J. Ramsay, A. V. Gopal, E. M. Gauger, A. Nazir, B. W. Lovett, A. M. Fox, and M. S. Skolnick, Phys. Rev. Lett. **104**, 017402 (2010).
[38] P. Kaer, T. R. Nielsen, P. Lodahl, A. P. Jauho, and J. Mørk, Phys. Rev. Lett. **104**, 157401 (2010).
[39] A. Debnath, C. Meier, B. Chatel, and T. Amand, Phys. Rev. B **86**, 161304 (2012).
[40] P. R. Eastham, A. O. Spracklen, and J. Keeling, Phys. Rev. B **87**, 195306 (2013).
[41] P.-L. Ardelt, L. Hanschke, K. A. Fischer, K. Müller, A. Kleinkauf, M. Koller, A. Bechtold, T. Simmet, J. Wierzbowski, H. Riedl, G. Abstreiter, and J. J. Finley, Phys. Rev. B **90**, 241404 (2014).
[42] A. Nazir and D. P. S. McCutcheon, J. Phys. Condens. Matter **28**, 103002 (2016).
[43] D. P. S. McCutcheon and A. Nazir, New J. Phys. **12**, 113042 (2010).
[44] C. Roy and S. Hughes, Phys. Rev. B **85**, 115309 (2012).
[45] P. Kaer, T. R. Nielsen, P. Lodahl, A.-P. Jauho, and J. Mørk, Phys. Rev. B **86**, 085302 (2012).
[46] R. Manson, K. Roy-Choudhury, and S. Hughes, Phys. Rev. B **93**, 155423 (2016).

[47] R. Loudon, *The Quantum Theory of Light*, 2nd ed. (Oxford Science Publications, Oxford, 1973).
[48] M. Glässl, M. D. Croitoru, A. Vagov, V. M. Axt, and T. Kuhn, Phys. Rev. B **84**, 125304 (2011).
[49] S. Hughes and H. J. Carmichael, New J. Phys. **15**, 053039 (2013).
[50] M. Glässl, A. M. Barth, K. Gawarecki, P. Machnikowski, M. D. Croitoru, S. Lüker, D. E. Reiter, T. Kuhn, and V. M. Axt, Phys. Rev. B **87**, 085303 (2013).
[51] D. E. Reiter, T. Kuhn, M. Glässl, and V. M. Axt, J. Phys. Condens. Matter **26**, 423203 (2014).
[52] J. H. Quilter, A. J. Brash, F. Liu, M. Glässl, A. M. Barth, V. M. Axt, A. J. Ramsay, M. S. Skolnick, and A. M. Fox, Phys. Rev. Lett. **114**, 137401 (2015).
[53] S. Bounouar, M. Müller, A. M. Barth, M. Glässl, V. M. Axt, and P. Michler, Phys. Rev. B **91**, 161302 (2015).
[54] A. M. Barth, S. Lüker, A. Vagov, D. E. Reiter, T. Kuhn, and V. M. Axt, Phys. Rev. B **94**, 045306 (2016).
[55] A. J. Ramsay, T. M. Godden, S. J. Boyle, E. M. Gauger, A. Nazir, B. W. Lovett, A. M. Fox, and M. S. Skolnick, Phys. Rev. Lett. **105**, 177402 (2010).
[56] A. Vagov, M. Glässl, M. D. Croitoru, V. M. Axt, and T. Kuhn, Phys. Rev. B **90**, 075309 (2014).
[57] M. Glässl, L. Sörgel, A. Vagov, M. D. Croitoru, T. Kuhn, and V. M. Axt, Phys. Rev. B **86**, 035319 (2012).
[58] F. Liu, L. M. P. Martins, A. J. Brash, A. M. Barth, J. H. Quilter, V. M. Axt, M. S. Skolnick, and A. M. Fox, Phys. Rev. B **93**, 161407(R) (2016).
[59] A. J. Brash, L. M. P. P. Martins, A. M. Barth, F. Liu, J. H. Quilter, M. Glässl, V. M. Axt, A. J. Ramsay, M. S. Skolnick, and A. M. Fox, J. Opt. Soc. Am. B **33**, C115 (2016).